



## Frontiers in Heat and Mass Transfer

Available at [www.ThermalFluidsCentral.org](http://www.ThermalFluidsCentral.org)



# FLOW OVER AN EXPONENTIALLY STRETCHING SHEET WITH HALL, THERMAL RADIATION AND CHEMICAL REACTION EFFECTS

D. Srinivasacharya\*, P. Jagadeeshwar

*Department of Mathematics, National Institute of Technology, Warangal - 506004, India*

### ABSTRACT

Numerical solutions for the boundary layer flow, heat and mass transfer of a viscous incompressible fluid over an exponentially stretching sheet is developed. The effect of Hall current, chemical reaction and thermal radiation are taken into account. Through similarity transformations, the governing boundary layer equations are reduced to a set of coupled non-linear ordinary differential equations and then linearized using the successive linearization method. The resultant linear system is solved using the Chebyshev pseudo spectral method. The numerical results for velocity, temperature and concentration are shown graphically. The skin-frictions are calculated and variations with pertinent parameters are presented in tabular form. Finally, a comparative analysis is conducted between the present results and known results in the literature for the special cases, and are found to be in good agreement.

**Keywords:** Hall Current, Thermal Radiation and Chemical Reaction.

## 1. INTRODUCTION

The study of heat and mass transfer over stretching surfaces is one of the important research area due to its significant use in various applications such as wire drawing, paper production, glass fiber, crystal growth, filaments spinning, food processing, continuous casting. Following the pioneering works of Sakiadis (1961a, 1961b) on the flow due to a stretching sheet, several researchers (Crane 1968, Aziz 2008, Bhattacharya 2011, Bachak *et al.* 2012, Mandal and Mukhopadhyay 2013, Kumari and Nath 2014, Srinivasacharya and Jagadeeshwar 2017) considered this flow problem including the heat and mass transfer analysis under various physical situations. In contemporary years, the study of magnetohydrodynamic (MHD) flow problems has gained considerable attention of the researchers because of its applications in several engineering disciplines. The cooling of filaments or continuous strips and thinning and annealing of copper wires are the part of process of most of metallurgical industries, which are generally stretched during the process. Once these are brought into an electrically conducting fluid which is exposed to a strong magnetic field, the cooling rate can be adjusted so that the final product can be achieved with desired characteristics. Several researchers analyzed the MHD flow, heat and mass transfer over a stretching surface in Newtonian and non-Newtonian fluids with various effects. When the strong magnetic field is utilized the effect of Hall current is very predominant. The study of effects of Hall current on MHD flows has been given much importance due to its widely spread applications in power generators and pumps, Hall accelerators, electric transformers, refrigeration coils, flight MHD, solar physics in the sunspot development, the solar cycle, the structure of magnetic stars, cool combustors, electronic system cooling, thermal energy storage, fiber and granular insulation, oil extraction and flow through filtering devices and porous material regenerative heat exchangers. El-Aziz (2010) studied the effect of Hall currents on the flow and heat transfer of an electrically conducting fluid over an unsteady stretching surface in presence of a strong magnetic field. Shateyi and Motsa (2011) considered the MHD boundary layer flow over an unsteady stretching surface in presence of Hall currents. Srinivasacharya and Kaladhar

(2012) mentioned in their investigation that the fluid tangential velocity and temperature are increasing and the induced cross flow velocity is decreasing as the Hall parameter increases. Su and Zheng (2013) investigated the influence of Hall current and velocity slip effects on the flow and rate of heat transfer of nanofluid. Recently, Srinivasacharya and Jagadeeshwar (2017) reported the effect of Joule heating on the MHD boundary layer flow on an exponentially stretching surface with Hall current and velocity slip at the boundary.

The effect of thermal radiation on convective flows have applications in physics and engineering such as space technology, solar power technology, propulsion devices for aircraft and other industrial areas. Qasim (2011) analyzed the MHD flow and heat transfer over a permeable stretching sheet in the presence of thermal radiation and Ohmic dissipation. Kameswaran *et al.* (2012) analyzed the effect of radiation on MHD Newtonian fluid over an exponentially stretching sheet. Mukhopadhyay and Gorla (2012) investigated the influence of partial slip and thermal radiation on boundary layer flow past a permeable exponential stretching sheet. Seini and Makinde (2013) studied the MHD boundary layer flow due to exponential stretching sheet in the presence of radiation and chemical reaction. Hussain *et al.* (2014) explained the radiative hydromagnetic flow of Jeffrey nanofluid by an exponentially stretching sheet. Mabood *et al.* (2014) studied the analytical solution for the flow of a viscous incompressible MHD fluid in presence of radiation towards an exponentially stretching sheet. Santosh *et al.* (2015) analyzed the thermal radiation effects on MHD boundary layer flow over an exponentially stretching surface. Ibrahim and Shankar (2016) investigated the effect of thermal radiation on MHD boundary layer flow and heat transfer past a stretching sheet embedded in non-Darcian porous medium. Recently, Umshaiah *et al.* (2017) reported the nonlinear radiative heat transfer to carreau fluid over a nonlinear stretching sheet in a porous medium and with viscous dissipation.

The study of heat and mass transfer with chemical reaction has received considerable attention because of its importance in chemical and hydro-metallurgical industries such as design of chemical processing equipment, polymer production, the manufacturing of ceramics or glassware etc. Zaib and Shafie (2014) studied the effect of Hall currents

\* Corresponding author Email: [dsc@nitw.ac.in](mailto:dsc@nitw.ac.in), [dsrinivasacharya@yahoo.com](mailto:dsrinivasacharya@yahoo.com)

with Soret and Dufour effects on unsteady MHD flow over an unsteady stretching surface with Joule heating and viscous dissipation with thermal stratification, chemical reaction. Das (2014) investigated the effect of chemical reaction and viscous dissipation on MHD mixed convective heat and mass transfer flow of second grade fluid past a semi-infinite stretching sheet in the presence of thermal diffusion and thermal radiation. Murthy *et al.* (2015) presented the influence of the prominent viscous dissipation and chemical reaction effects on boundary layer stagnation point flow past a stretching/shrinking sheet in a nanofluid.

The aim of the present work is to analyze the combined effects of Hall current, thermal radiation and chemical reaction over an exponential stretching surface in the presence of strong magnetic field subject to velocity slip and suction or injection.

## 2. MATHEMATICAL FORMULATION

Consider a steady electrically conducting flow of incompressible viscous fluid (with temperature  $T_\infty$  and concentration  $C_\infty$ ) past a stretching sheet with temperature  $T_w(x)$  and concentration  $C_w(x)$ . Choose the coordinate system such that the positive  $x$ -axis is taken along the sheet in the direction of flow,  $y$ -axis is perpendicular to the sheet in the outward direction of the flow and  $z$ -axis coincides with the leading edge of the sheet. The sheet velocity varies as an exponential function of the distance  $x$  from the slit. A strong magnetic field of strength  $B(x)$  is applied in  $y$ -direction and the influence of Hall current is included. The induced magnetic field is ignored as the magnetic Reynolds number is very low. The flow is three dimensional in view of the cross flow in the  $z$ -direction induced by the presence of Hall current. The velocity vector is  $(u, v, w)$ , the temperature is  $T$  and the concentration is  $C$ . The fluid is considered to be a gray, absorbing/emitting radiation, but non-scattering medium. The Rosseland approximation (Sparrow and Cess 1978) is used to describe the radiative heat flux in the energy equation. Also, it is assumed that there exists a homogenous chemical reaction of the first order with rate constant  $k_1$  between the diffusing species and the fluid.

With the above assumptions together with the Boussinesq and the boundary layer approximations, the equations governing the present flow problem are given by

$$u \frac{\partial u}{\partial x} + v \frac{\partial v}{\partial y} = 0 \quad (1)$$

$$u \frac{\partial u}{\partial x} + v \frac{\partial u}{\partial y} = \nu \frac{\partial^2 u}{\partial y^2} + g\beta_T(T - T_\infty) + g\beta_C(C - C_\infty) - \frac{\sigma B^2}{\rho(1 + \beta_h^2)}(u + \beta_h w) \quad (2)$$

$$u \frac{\partial w}{\partial x} + v \frac{\partial w}{\partial y} = \nu \frac{\partial^2 w}{\partial y^2} + \frac{\sigma B^2}{\rho(1 + \beta_h^2)}(\beta_h u - w) \quad (3)$$

$$u \frac{\partial T}{\partial x} + v \frac{\partial T}{\partial y} = \alpha \frac{\partial^2 T}{\partial y^2} + \frac{16T_\infty^3 \sigma^*}{3k^* \rho c_p} \frac{\partial^2 T}{\partial y^2} \quad (4)$$

$$u \frac{\partial C}{\partial x} + v \frac{\partial C}{\partial y} = D \frac{\partial^2 C}{\partial y^2} - k_1(C - C_\infty) \quad (5)$$

where  $\rho$  is density,  $c_p$  is specific heat at the constant pressure,  $g$  is the acceleration due to gravity,  $\mu$  is the dynamic viscosity of the fluid,  $\nu$  is the kinematic viscosity of the fluid,  $\beta_h$  is Hall parameter,  $\alpha$  is the thermal diffusivity,  $\sigma^*$  is the Stefan-Boltzmann constant,  $k^*$  is the mean absorption coefficient and  $D$  is the mass diffusivity. Boundary conditions are

$$\left. \begin{aligned} u &= U + Nv \frac{\partial u}{\partial y}, v = -V(x), w = 0, T_w = T_\infty + T_0 e^{\frac{2x}{L}}, C_w = C_\infty + C_0 e^{\frac{2x}{L}} \text{ at } y=0 \\ u &\rightarrow 0, w \rightarrow 0, T \rightarrow T_\infty, C \rightarrow C_\infty \text{ as } y \rightarrow \infty \end{aligned} \right\} \quad (6)$$

Here  $B(x) = B_0 e^{\nu 2L}$  is magnetic field term and  $B_0$  is the constant magnetic field,  $U = U_0 e^{\nu L}$  is stretching velocity and  $U_0$  is reference velocity,  $V = V_0 e^{\nu 2L}$  is the special velocity at the wall and  $V_0$  is the initial strength of suction,  $N = N_0 e^{-\nu 2L}$  is the velocity slip factor which changes with  $x$  and  $N_0$  is the initial value of the velocity slip factor,  $k_1 = k_0 e^{\nu L}$  is the exponential chemical reaction rate and  $k_0$  is the constant,  $V(x) > 0$  is the velocity of suction and  $V(x) < 0$  is the velocity of injection. If we take  $N = 0$ , no slip case can be achieved.

Introducing the following Similarity variables

$$\left. \begin{aligned} \eta &= y \sqrt{\frac{U_0}{2\nu L}} e^{\frac{x}{2L}}, \psi = \sqrt{2\nu L U_0} e^{\frac{x}{2L}} f, \\ u &= U_0 e^{\frac{x}{L}} f', v = -\sqrt{\frac{\nu U_0}{2L}} e^{\frac{x}{2L}} (f + \eta f'), \\ w &= U_0 e^{\frac{x}{L}} g, T = T_\infty + T_0 e^{\frac{2x}{L}} \theta(\eta), C = C_\infty + C_0 e^{\frac{2x}{L}} \phi(\eta) \end{aligned} \right\} \quad (7)$$

into Eqs. (1) - (5), we obtain

$$f''' + ff'' - 2f'^2 + 2Ri(\theta + \mathbb{B}\phi) - \frac{Ha}{1 + \beta_h^2}(f' + \beta_h g) = 0 \quad (8)$$

$$g'' - 2f'g + fg' + \frac{Ha}{1 + \beta_h^2}(\beta_h f' - g) = 0 \quad (9)$$

$$\left(1 + \frac{4R}{3}\right)\theta'' + Pr(f\theta' - 4f'\theta) = 0 \quad (10)$$

$$\phi'' + Sc(f\phi' - 4f'\phi) - Sc\gamma\phi = 0 \quad (11)$$

where the prime denotes differentiation with respect to  $\eta$ ,  $Pr = \nu/\alpha$  is the Prandtl number,  $Sc = \nu/D$  is the Schmidt number,  $S = V_0 \sqrt{2L/\nu U_0}$  is the suction/injection parameter according as  $S > 0$  or  $S < 0$  respectively,  $\lambda = N_0 \sqrt{\nu U_0}/2L$  is the velocity slip parameter,  $Re = U_0 L/\nu$  is the Reynolds's number,  $Gr = g\beta_T TL^3/\nu^2$  is the Grashof number,  $Ri = Gr/Re^2$  is the Richardson number (mixed convection parameter),  $Ha = 2L\sigma B_0^2/\rho U_0$  is the magnetic parameter,  $\mathbb{B} = \beta_c C_0/\beta_T T_0$  is the buoyancy ratio,  $R = 4\sigma^* T_\infty^3/\kappa\kappa^*$  is the radiation parameter and  $\gamma = 2Lk_0/U_0$  is the chemical reaction parameter.

The corresponding boundary conditions reduce to

$$\left. \begin{aligned} f(0) &= S, f'(0) = 1 + \lambda f''(0), g(0) = 0, \theta(0) = 1, \phi(0) = 1 \text{ at } \eta = 0 \\ f'(\infty) &\rightarrow 0, g(\infty) \rightarrow 0, \theta(\infty) \rightarrow 0, \phi(\infty) \rightarrow 0 \text{ as } \eta \rightarrow \infty \end{aligned} \right\} \quad (12)$$

Results of practical interest are the wall shear stress in  $x$  and  $z$ -directions, heat and mass transfer rates, respectively, acting on the stretching surface. The local skin-friction in  $x$ -direction  $C_{fx} = \frac{2\tau_{\omega x}}{\rho U^2}$ , the local

skin-friction in  $z$ -direction  $C_{fz} = \frac{2\tau_{\omega z}}{\rho U^2}$ , the local Nusselt number

$$Nu_x = \frac{xq_w}{k(T_w - T_\infty)} \text{ and local Sherwood number } Sh_x = \frac{xq_m}{k(C_w - C_\infty)},$$

are given by

$$f''(0) = \sqrt{\frac{L}{2x}} Re_x^{\frac{1}{2}} C_{fx}, g'(0) = \sqrt{\frac{L}{2x}} Re_x^{\frac{1}{2}} C_{fz},$$

$$-\left(1 + \frac{4R}{3}\right) \theta'(0) = \sqrt{\frac{2L}{x}} Re_x^{\frac{1}{2}} Nu_x \quad \text{and} \quad -\phi'(0) = \sqrt{\frac{2L}{x}} Re_x^{\frac{1}{2}} Sh_x$$

(13)

where  $Re_x = \frac{xU(x)}{\nu}$  is the local Reynolds number.

### 3. METHOD OF SOLUTION

The successive linearisation method (SLM) (Motsa and Shateyi 2006, Awad *et al.* 2011) is used to linearize the system of differential equations (8)–(11). The resulting linearised system of equations are solved using the Chebyshev pseudo spectral method (Canuto *et al.* 2006). In SLM, the functions  $f(\eta)$ ,  $g(\eta)$ ,  $\theta(\eta)$  and  $\phi(\eta)$  are assumed to be expressed as

$$\left. \begin{aligned} f(\eta) &= f_r(\eta) + \sum_{i=0}^{r-1} f_i(\eta), g(\eta) = g_r(\eta) + \sum_{i=0}^{r-1} g_i(\eta), \\ \theta(\eta) &= \theta_r(\eta) + \sum_{i=0}^{r-1} \theta_i(\eta), \phi(\eta) = \phi_r(\eta) + \sum_{i=0}^{r-1} \phi_i(\eta) \end{aligned} \right\} \quad (14)$$

where  $f_r(\eta)$ ,  $g_r(\eta)$ ,  $\theta_r(\eta)$  and  $\phi_r(\eta)$  ( $r = 1, 2, 3, \dots$ ) are unknown functions and  $f_i(\eta)$ ,  $g_i(\eta)$ ,  $\theta_i(\eta)$  and  $\phi_i(\eta)$  ( $i \geq 1$ ) are approximations and are obtained by recursively solving the linear part of the system of equations that results from substituting Eq. (14) in the governing equations (8)–(11). The initial approximation  $f_0(\eta)$ ,  $g_0(\eta)$ ,  $\theta_0(\eta)$  and  $\phi_0(\eta)$  chosen so that they satisfy boundary conditions (12).

The succeeding solutions for  $f_r(\eta)$ ,  $g_r(\eta)$ ,  $\theta_r(\eta)$  and  $\phi_r(\eta)$  ( $r \geq 1$ ) are brought by recursively solving the below linearized system of ordinary differential equations

$$f''_{r+1} + a_{1,r-1} f''_r + a_{2,r-1} f'_r + a_{3,r-1} f_r - (a \beta_h) g_r + (2 Ri) \theta_r + (2 \mathbb{B} Ri) \phi_r = \mathcal{E}_{1,r-1} \quad (15)$$

$$b_{1,r-1} f'_r + b_{2,r-1} f_r + g''_r + b_{3,r-1} g'_r + b_{4,r-1} g_r = \mathcal{E}_{1,r-1} \quad (16)$$

$$c_{1,r-1} f'_r + c_{2,r-1} f_r + b \theta''_r + c_{3,r-1} \theta'_r + c_{4,r-1} \theta_r = \mathcal{E}_{3,r-1} \quad (17)$$

$$d_{1,r-1} f'_r + d_{2,r-1} f_r + \phi''_r + d_{3,r-1} \phi'_r + d_{4,r-1} \phi_r = \mathcal{E}_{4,r-1} \quad (18)$$

where the coefficients  $a_{k,r-1}, b_{k,r-1}, c_{k,r-1}, d_{k,r-1}$  and  $\mathcal{E}_{k,r-1}$ , ( $k = 1, 2, 3, 4$ ) are in terms of the approximations  $f_i, g_i, \theta_i$  and  $\phi_i$ , ( $i = 1, 2, 3, \dots, n-1$ ) and their derivatives.

The associated boundary conditions are

$$f_r(0) = \lambda f_r'(0) - f_r'(0) = f_r'(\infty) = g_r(0) = g_r(\infty) = \theta_r(0) = \theta_r(\infty) = \phi_r(0) = \phi_r(\infty) = 0 \quad (19)$$

Hence,  $f(\eta)$ ,  $g(\eta)$ ,  $\theta(\eta)$  and  $\phi(\eta)$  are obtained as

$$f(\eta) \approx \sum_{i=0}^M f_i(\eta), g(\eta) \approx \sum_{i=0}^M g_i(\eta), \theta(\eta) \approx \sum_{i=0}^M \theta_i(\eta), \phi(\eta) \approx \sum_{i=0}^M \phi_i(\eta) \quad (20)$$

where  $M$  is the order of SLM approximation.

The linearized equations (15) to (18) are solved using Chebyshev spectral collocation method (Canuto *et al.* 2006). The problem is solved for  $[0, L]$  instead of  $[0, \infty)$ , where the parameter  $L$  is used to recover the conditions at infinity. To apply this method the domain under consideration  $[0, L]$  is

transformed to  $[-1, 1]$  by the transformation  $\xi = \frac{2\eta}{L} - 1, -1 \leq \xi \leq 1$ .

Approximating the functions  $f_r, g_r, \theta_r$  and  $\phi_r$  their derivatives in terms of Chebyshev interpolating polynomials at  $N+1$  Gauss-Lobatto

collocation points  $\xi_k = \cos \frac{\pi k}{N}, k = 0, 1, 2, \dots, N$  and substituting in (15)

(19) leads to the matrix equation (for details see Canuto *et al.* (2006)). Incorporating boundary conditions and solving the resulting matrix system, we get the solution.

### 4. RESULTS AND DISCUSSIONS

To validate the accuracy of the numerical method, results are obtained for particular values of  $Ri, Ha, S$  and  $\lambda$ . Table (1) provides the comparison between the results obtained for local skin-friction coefficient  $-f''(0)$  and  $f(\infty)$  by using the present method and numerical results obtained by Magyari and Keller (1999) and found to be in good agreement.

**Table 1** Comparison analysis for  $-f''(0)$  and  $f(\infty)$  calculated by the present method for  $S = 0, \lambda = 0, Ri = 0$  and  $Ha = 0$ .

	Magyari and Keller (1999)	Present
$-f''(0)$	1.281808	1.28180856
$f(\infty)$	0.905639	0.90564370

In order to analyze the influence of pertinent parameters, the numerical calculations are carried out by taking  $Pr = 1.0, Sc = 0.22, Ri = 1.0, \mathbb{B} = 0.5, S = 0.5, \lambda = 1.0, \beta_h = 1.0, Ha = 2.0, R = 0.5, \gamma = 0.5, N = 100$  and  $L = 20$  unless otherwise mentioned.

Figures 1(a)–1(d) represent the variation of the velocities, temperature and concentration with  $S$ . It is seen from these figures that the velocities, temperature and concentration are increasing with increase in the injection ( $S < 0$ ). It is also observed that the suction ( $S > 0$ ) reduces both the momentum, thermal and concentration boundary layer thickness which, in turn, reduce the velocity, temperature and concentration.

The influence  $Ri$  on the velocities, temperature and concentration is depicted in figures 2(a)–2(d). From figure 2(a), it is noticed that the tangential velocity is enhanced with increase in the values of  $Ri$ . This is because, a favorable pressure gradient is induced as a result of the positive values of  $Ri$  which, in turn, increases the fluid flow. The same effect is observed for the secondary velocity as shown in the figure 2(b). From the figures 2(c)–2(d), it is understood that the temperature and the concentration are decreasing with increasing values of  $Ri$ . This is due to the fact that positive values of  $Ri$  accelerates the fluid and results in decreasing both the thermal and concentration boundary layers.

The variation of the velocities, temperature and concentration for different values of  $Ha$  is shown in the figures 3(a)–3(d). It is evident from the figure 3(a), that the primary velocity is decreasing with increase in the values of  $Ha$ . The application of uniform magnetic field normal to flow direction gives rise to Lorentz force which has the tendency to slow down the velocity in the boundary layer. From figure 3(b), it is seen that there is no cross flow velocity when  $Ha = 0$  and it increases gradually with increase in  $Ha$ . Hence, for large values of  $Ha$ , a cross flow is generated due to the Hall effect. From figures 3(c)–3(d), it is clear that the temperature and concentration are increasing with increase in the value of magnetic parameter  $Ha$ .

Figures 4(a)–4(d) represent the behavior of the velocities, temperature and concentration with Hall parameter  $\beta_h$ . From figure 4(a), it is observed that the tangential velocity increases with increase in  $\beta_h$ . Figure 4(b) shows that the cross flow velocity increases with increase in the value of  $\beta_h$ . It is increasing near the plate and then gradually decreasing. Figures 4(c) and 4(d) depict that the temperature and concentration are diminishing with increase in the value of  $\beta_h$ .

The influence of  $\gamma$  on the velocities, temperature and concentration is presented in the figures 5(a)–5(d). Figure 5(a) depicts that the temperature is decreasing with increase in the values  $\gamma$ . The same effect is observed on the secondary velocity as presented in the figure 5(b). Further, from figure 5(c), it is seen that the temperature is rising with increase in the values of  $\gamma$ . The concentration is reduced with increasing values of  $\gamma$  as depicted in the figure 5(d). This is due to the fact that the reaction-rate parameter is a decelerating agent and the conversion of the species takes place as a result of chemical reaction and thereby reduces the concentration in the boundary layer and increases the thermal boundary layer thickness.

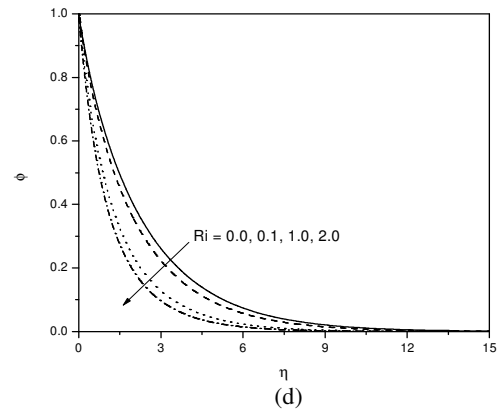
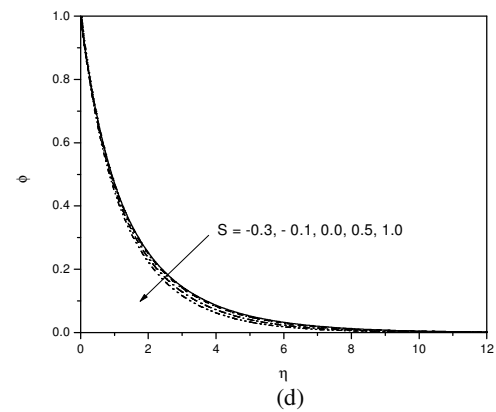
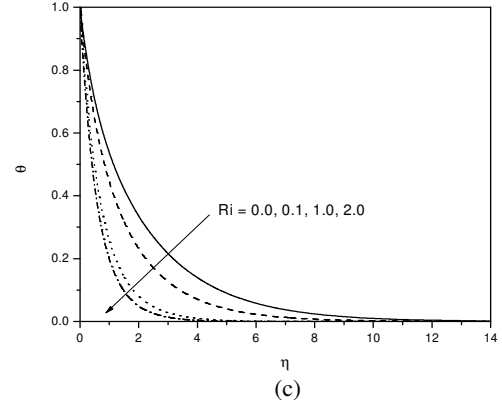
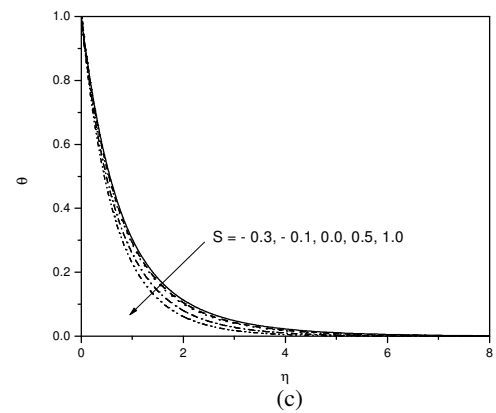
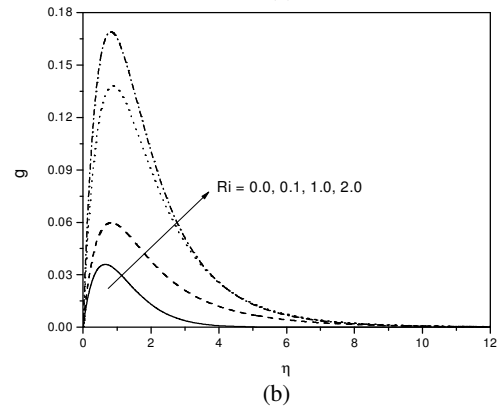
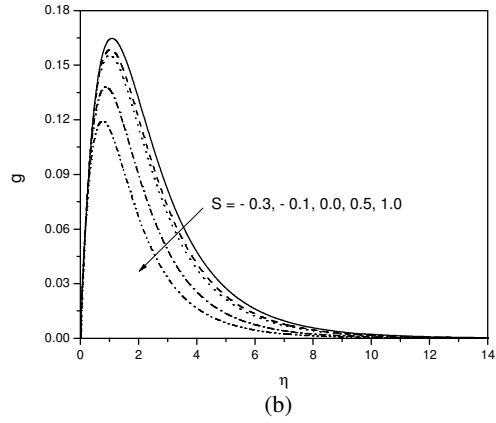
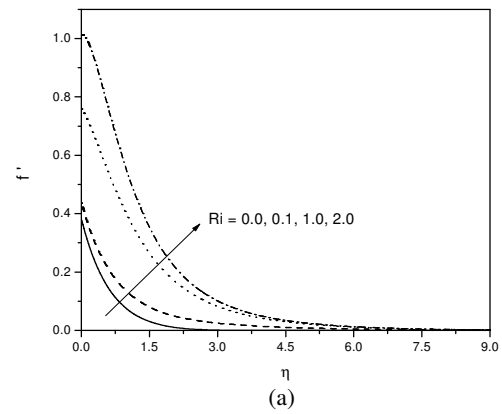
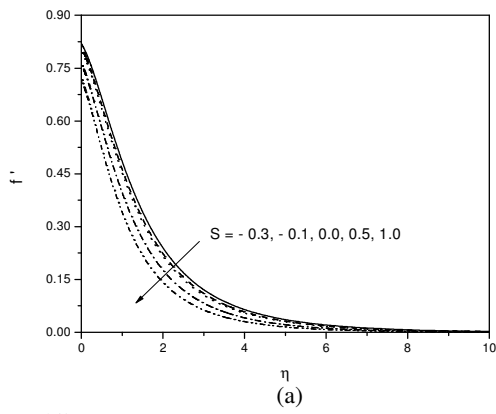


**Fig. 1** Effect of  $S$  on (a) velocity, (b) transverse velocity, (c) temperature and (d) concentration

**Fig. 2** Effect of  $Ri$  on (a) velocity, (b) transverse velocity, (c) temperature and (d) concentration

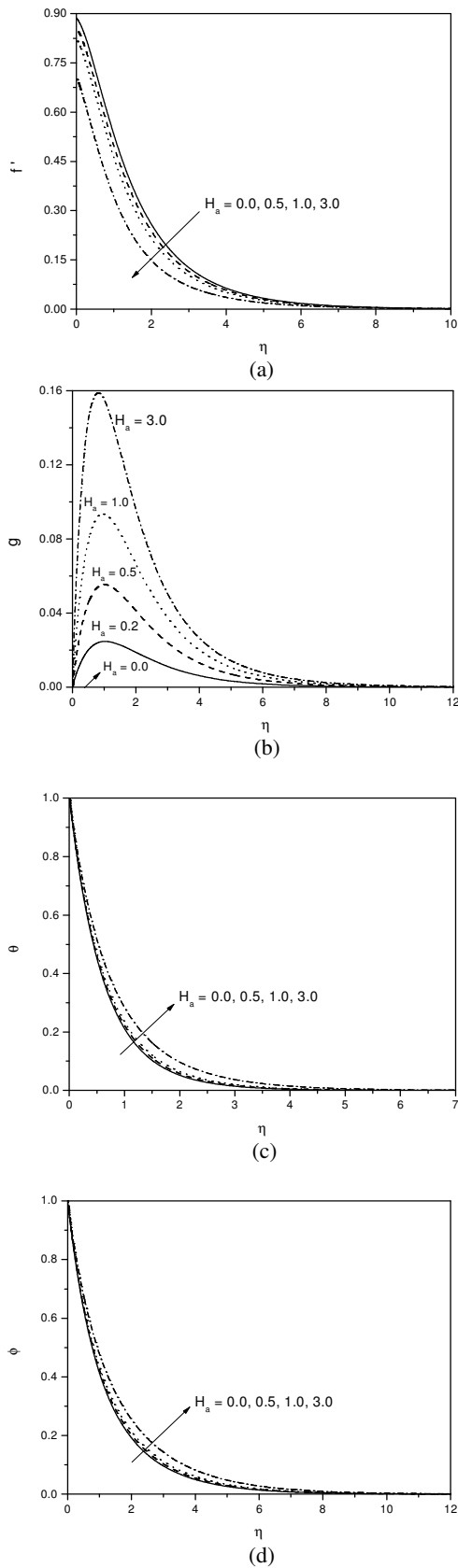


**Fig. 3** Effect of  $H_a$  on (a) velocity, (b) transverse velocity, (c) temperature and (d) concentration

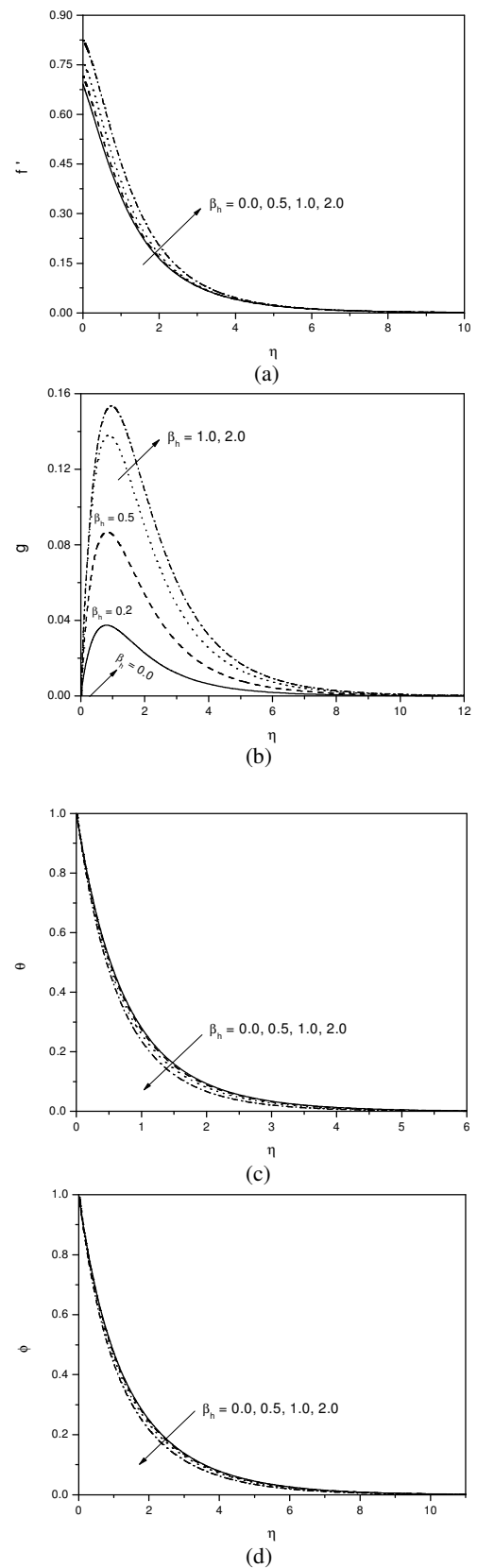


**Fig. 4** Effect of  $\beta_h$  on (a) velocity, (b) transverse velocity, (c) temperature and (d) concentration

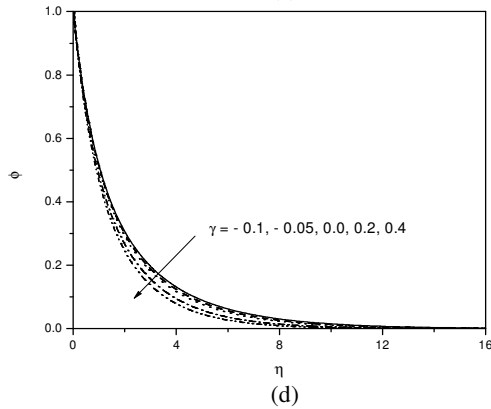
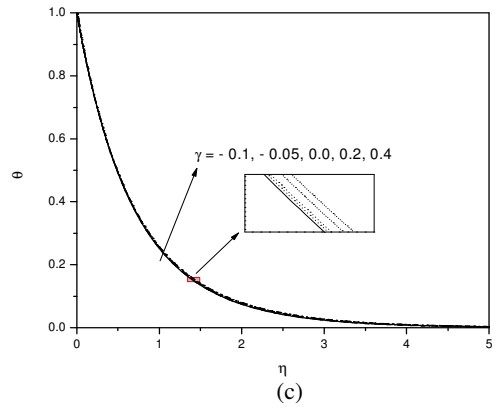
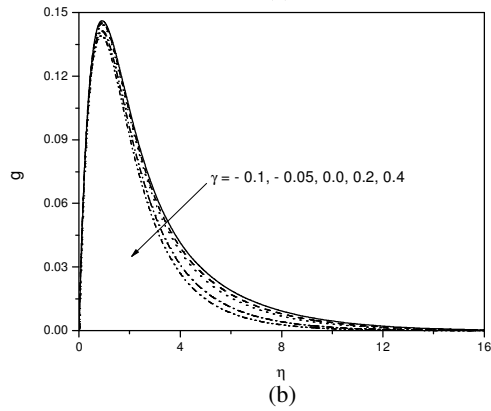
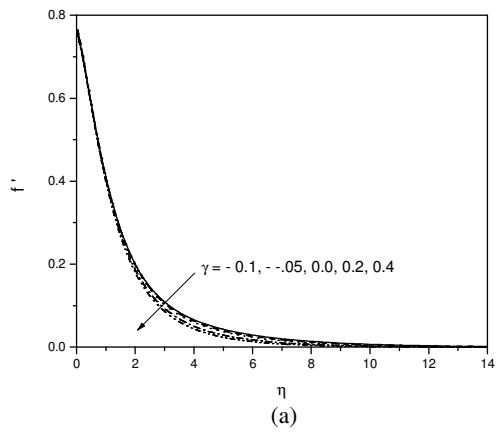


**Fig. 5** Effect of  $\gamma$  on (a) velocity, (b) transverse velocity, (c) temperature and (d) concentration

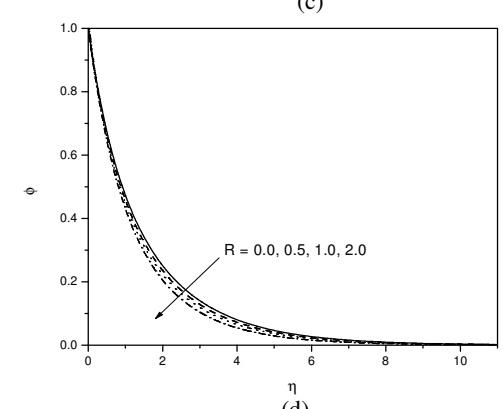
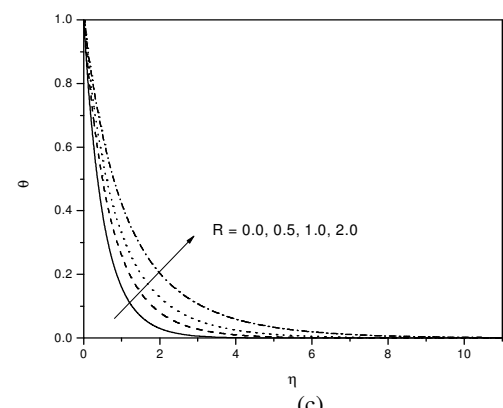
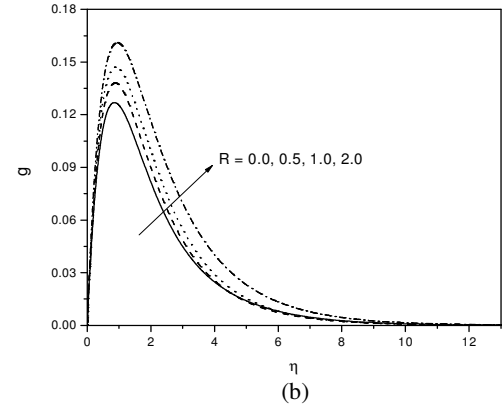
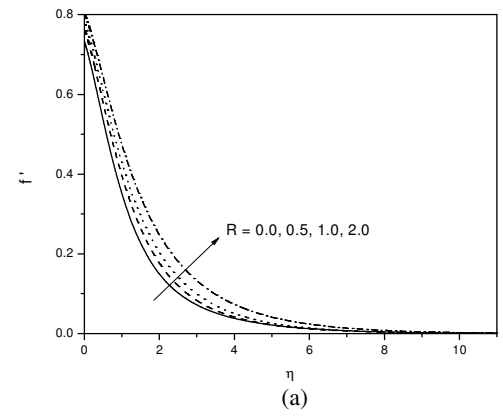


**Fig. 6** Effect of  $R$  on (a) velocity, (b) transverse velocity, (c) temperature and (d) concentration

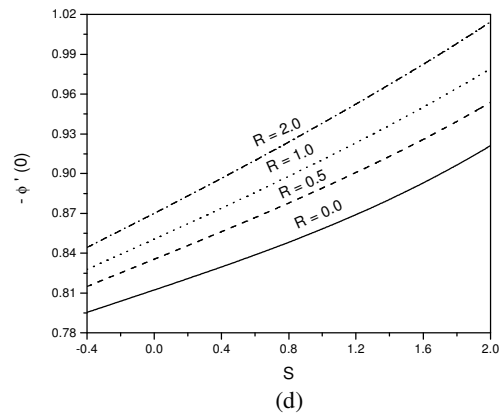
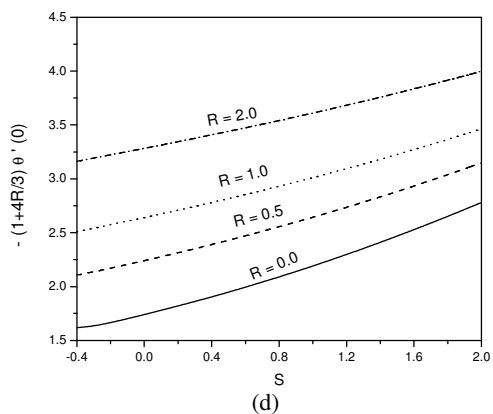
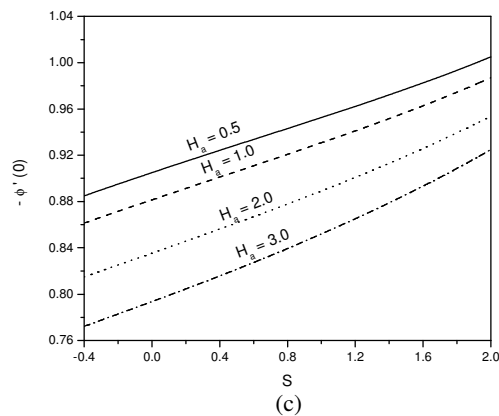
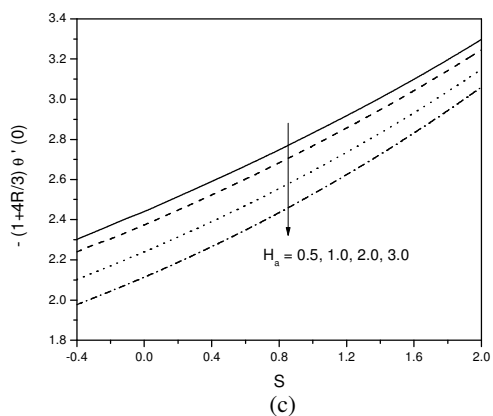
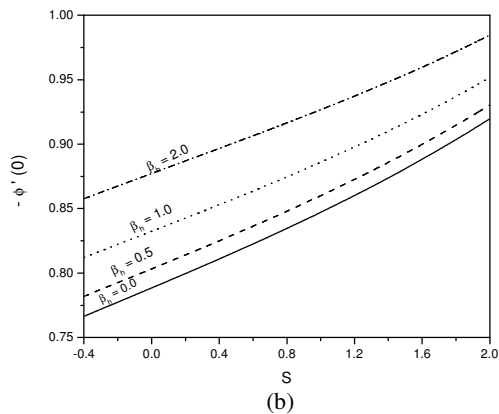
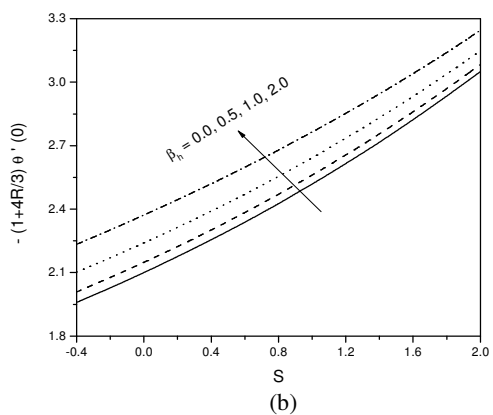
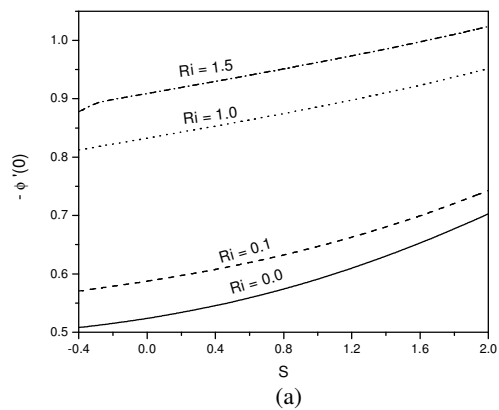
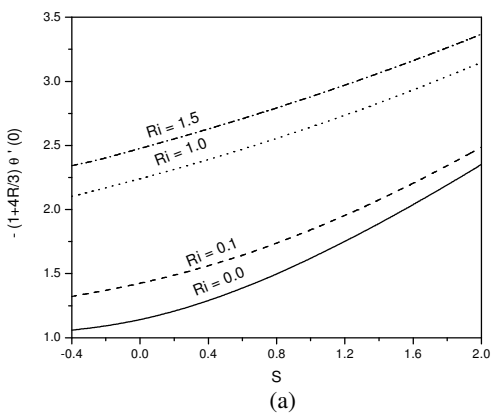


**Fig. 7** Effect of (a)  $Ri$ , (b)  $\beta_h$ , (c)  $H_a$  and (d)  $R$  on Nusselt number.

**Fig. 8** Effect of (a)  $Ri$ , (b)  $\beta_h$ , (c)  $H_a$  and (d)  $R$  on Sherwood number.

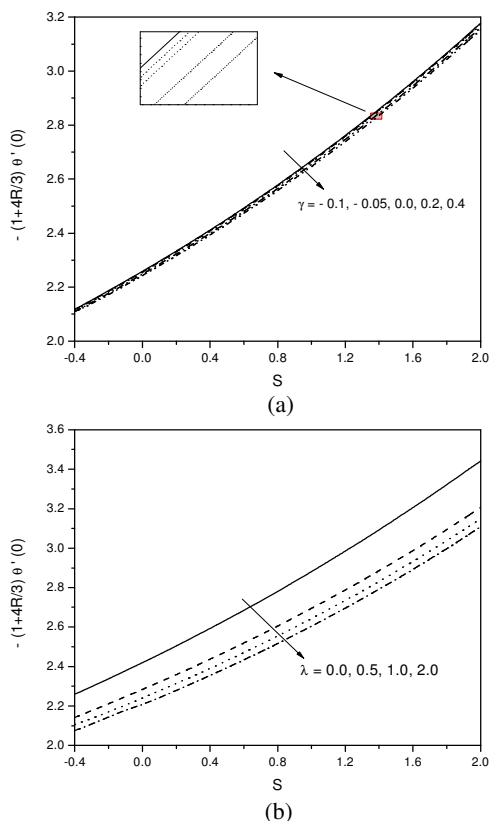


Fig. 9 Effect of (a)  $\gamma$  and (b)  $\lambda$  on Nusselt number.

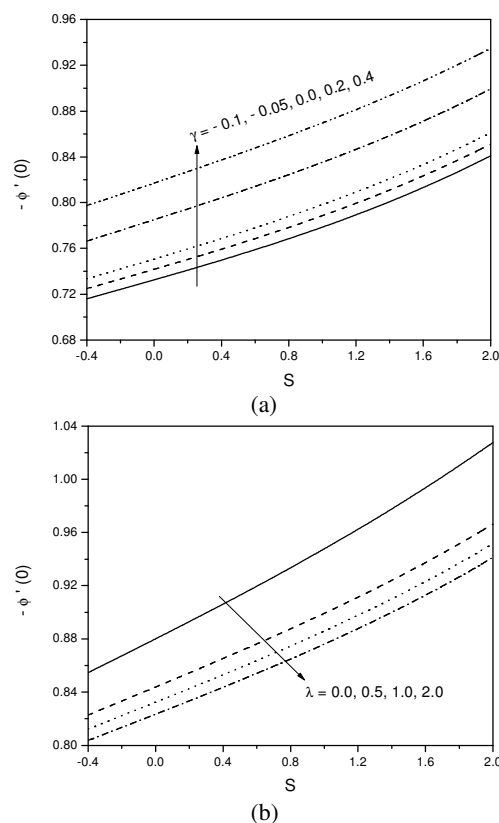


Fig. 10 Effect of (a)  $\gamma$  and (b)  $\lambda$  on Sherwood number.

The behaviour of both the velocities, temperature and concentration profiles with the radiation parameter  $R$  is exhibited in the figures 6(a)–6(d). From figures 6(a) and 6(b), it is observed that both the velocities are increasing with increase in the value of  $R$ . Applying the thermal radiation accumulates the momentum boundary layer thickness and hence, velocity rises. It is seen from the figure 6(c) that the temperature increases with increasing values of thermal radiation, which in turn, intensifies the thermal boundary layer thickness. Figure 6(d) shows that concentration is decreasing with thermal radiation.

The influence of  $Ri$ ,  $\beta_h$ ,  $H_a$ ,  $R$ ,  $\gamma$  and  $\lambda$  on the heat transfer ( $-\theta'(0)$ ) coefficient against  $S$  are presented in the figures 7(a)–7(d) and 9(a)–9(b), respectively. It is understood from the figures that heat transfer rate is increasing with  $S$ . It is observed from figures 7(a) and 7(b) that the heat transfer coefficient is increasing with mixed convection parameter  $Ri$  and Hall parameter  $\beta_h$ . On the other hand, the rate of heat transfer decreases with increase in the value of magnetic parameter  $H_a$ , as shown in the figure 7(c). It is evident from figure 7(d) that, the heat transfer rate is increasing with increase in the value of radiation parameter  $R$ . The heat transfer rate from the sheet to the fluid is decreasing with the increasing values of chemical reaction parameter  $\gamma$  as presented in the figure 9(a). It is seen from figures 9(b) that heat transfer from the sheet to the fluid is decreasing with increase in the values of  $\lambda$ . This is due to the fact that, slipperiness enhances the thermal boundary layer thickness.

The variation mass transfer ( $-\phi'(0)$ ) coefficient against  $S$  are presented in the figures 8(a)–8(d) and 10(a)–10(b), respectively. It clear from the figures that mass transfer rate is increasing with increase in  $S$ . Figures 8(a), 8(b) and 8(d) shows that mass transfer from the sheet to fluid is increasing with increase in the values of mixed convection, Hall and thermal radiation parameters, respectively. While increase in magnetic parameter decreases the rate of mass transfer as shown in the figure 8(c). Figures 10(a) and 10(b) shows the variation of mass transfer coefficient for different values of chemical reaction parameter  $\gamma$  and slip parameter  $\lambda$ . It is evident from these figures that increase in the value chemical reaction parameter, the mass transfer rate is increase. On the other hand, due to the slipperiness the mass transfer is decreased.

Table 2 Values of skin-friction coefficients  $f''(0)$  and  $g'(0)$  for different values of  $\lambda$ ,  $\beta_h$ ,  $H_a$ ,  $Ri$ ,  $R$  and  $\gamma$ .

$\lambda$	$\beta_h$	$H_a$	$Ri$	$R$	$\gamma$	$f''(0)$	$g'(0)$
0.0	1.0	2.0	1.0	0.5	0.5	-0.78606115	0.49875513
0.5	1.0	2.0	1.0	0.5	0.5	-0.34456759	0.46291098
1.0	1.0	2.0	1.0	0.5	0.5	-0.22173409	0.45234859
2.0	1.0	2.0	1.0	0.5	0.5	-0.12964196	0.44424225
1.0	0.0	2.0	1.0	0.5	0.5	-0.29327814	0.00000000
1.0	0.1	2.0	1.0	0.5	0.5	-0.29212505	0.06899147
1.0	0.5	2.0	1.0	0.5	0.5	-0.26825492	0.30509370
1.0	2.0	2.0	1.0	0.5	0.5	-0.15664931	0.45387080
1.0	1.0	0.0	1.0	0.5	0.5	-0.09196649	0.00000001
1.0	1.0	0.1	1.0	0.5	0.5	-0.09855922	0.03411152
1.0	1.0	1.0	1.0	0.5	0.5	-0.15866424	0.27790055
1.0	1.0	3.0	1.0	0.5	0.5	-0.27779617	0.56376751
1.0	1.0	2.0	0.0	0.5	0.5	-0.61660061	0.15023781
1.0	1.0	2.0	0.5	0.5	0.5	-0.38724236	0.35088076
1.0	1.0	2.0	1.5	0.5	0.5	-0.08245520	0.52482100
1.0	1.0	2.0	3.0	0.5	0.5	0.25675371	0.67201110
1.0	1.0	2.0	1.0	0.0	0.5	-0.24877696	0.42396587
1.0	1.0	2.0	1.0	0.5	0.5	-0.22173409	0.45234859
1.0	1.0	2.0	1.0	1.0	0.5	-0.20530645	0.47190037
1.0	1.0	2.0	1.0	2.0	0.5	-0.18538544	0.49777051
1.0	1.0	2.0	1.0	0.5	-1.0	-0.20496139	0.46994562
1.0	1.0	2.0	1.0	0.5	-0.5	-0.21198405	0.47034472
1.0	1.0	2.0	1.0	0.5	0.0	-0.21753173	0.46012738
1.0	1.0	2.0	1.0	0.5	1.0	-0.22504567	0.44718366
1.0	1.0	2.0	1.0	0.5	2.0	-0.23024909	0.44017046



The behaviour of  $f''(0)$  and  $g'(0)$  for different values of  $\lambda$ ,  $\beta_h$ ,  $H_a$ ,  $Ri$ ,  $R$  and  $\gamma$  are tabulated in Table (2). It is evident from the table that  $f''(0)$  is raising and  $g'(0)$  reducing with slipperiness. In presence of Hall parameter both the skin-frictions are increasing. It is also observed that when  $\beta_h = 0$ , then there is no secondary flow velocity and hence there's no skin-friction in  $z$ -direction. Table (2) illustrates that,  $f''(0)$  is decreasing and  $g'(0)$  is increasing with magnetic parameter. It is also seen that the skin-friction in  $z$ -direction is zero when  $H_a = 0$ . The positive values of  $Ri$  increases both the skin-frictions. In addition to this,  $f''(0)$  in  $x$ -direction is greatly increased with positive values of  $Ri$ . Furthermore, it is also identified that a unique value of  $f''(0) = -0.61660061$  and  $g'(0) = 0.15023781$  is attained when  $Ri = 0$  (the case of forced convection flow) and for all values of radiation parameter  $R$ . Because (8) and (10) are uncoupled when  $Ri = 0$ . As a result, the flow and thermal fields are independent. Hence, there's no effect of thermal field parameters on the flow field. On other hand, radiation parameter increases both the skin-frictions. At the end of the table the influence of chemical reaction parameter is presented. It is noticed from the table that,  $f''(0)$  is increasing and  $g'(0)$  is decreasing with  $\gamma < 0$  (destructive chemical reaction) and both are decreasing with  $\gamma > 0$  (constructive chemical reaction).

### 5. CONCLUSION

Viscous flow over an exponentially stretching sheet with Hall, thermal radiation and chemical reaction effects is studied. The governing equations are linearized using the successive linearization method and then the resulting linear differential equations are solved using the Chebyshev spectral collocation method. The following are the important findings from this study:

- Increasing the values of injection, mixed convection, Hall and thermal radiation parameters the primary velocity increase and reverse trend is observed for suction and magnetic and chemical reaction parameters.
- The secondary velocity increases with increase in the values of injection, mixed convection, magnetic, Hall and thermal radiation parameters. But decreases with increase in the values of suction and chemical reaction parameters.
- In the presence of injection, magnetic, chemical reaction and radiation parameters, temperature is increasing. While the temperature is decreasing with increase in the values of suction, mixed convection and Hall parameters.
- The heat transfer rate is increased with increase in the values of suction, mixed convection, radiation and Hall parameters while decreasing with all other parameters.
- The rate of mass transfer from the sheet to the fluid is decreasing by increasing the values of magnetic and slip parameters. But increasing, in all other cases.

### NOMENCLATURE

$\rho$	the density,
$c_p$	the specific heat at the constant pressure,
$g$	the acceleration due to gravity,
$\mu$	the dynamic viscosity of the fluid,
$\nu$	the kinematic viscosity of the fluid,
$\beta_h$	the Hall parameter,
$\alpha$	the thermal diffusivity,
$\sigma^*$	the Stefan-Boltzmann constant,
$k^*$	the mean absorption coefficient
$D$	the mass diffusivity.
$B_0$	the constant magnetic field,
$U_0$	the reference velocity,
$V_0$	the initial strength of suction,

$N_0$	the initial value of the velocity slip factor,
$k_0$	the constant,
$Pr$	the Prandtl number,
$Sc$	the Schmidt number,
$S$	the suction/injection parameter,
$A$	the velocity slip parameter,
$Re$	the Reynolds's number,
$Gr$	the Grashof number,
$Ri$	the Richardson number (mixed convection parameter),
$H_a$	the magnetic parameter,
$\mathbb{B}$	the buoyancy ratio,
$R$	the radiation parameter
$\gamma$	the chemical reaction parameter.
$C_{fx}$	the local skin-friction in x-direction
$C_{fz}$	the local skin-friction in z-direction
$Nu_x$	the local Nusselt number
$Sh_x$	local Sherwood number
$Re_x$	the local Reynolds number.

### REFERENCES

- Awad, F.G., Sibanda, P., Motsa S.S and Makinde, O.D., 2011, "Convection from an Inverted Cone in a Porous Medium with Cross Diffusion Effects," *Computers and Mathematics with Applications*, **61**, 1431-1441.  
<https://doi.org/10.1016/j.camwa.2011.01.015>
- Bachok, N., Ishak, A. and Pop, I., 2012, "Boundary Layer Stagnation-Point Flow and Heat Transfer over an Exponentially Stretching/Shrinking Sheet in a Nanofluid," *International Journal of Heat and Mass Transfer*, **55**, 8122-8128.  
<https://doi.org/10.1016/j.ijheatmasstransfer.2012.08.051>
- Bhattacharyya, K., 2011, "Boundary Layer Flow and Heat Transfer over an Exponentially Shrinking Sheet," *Chin. Phys. Lett.*, **28**(7), Article ID 074701, 1-4.  
<http://stacks.iop.org/0256-307X/28/i=7/a=074701>
- Canuto, C., Hussaini, M.Y., Quarteroni A., and Zang, T.A., 2006, *Spectral Methods in Fluid Dynamics*, Springer, Berlin, Germany.
- Das, K., 2014., "Influence of Chemical Reaction and Viscous Dissipation on MHD Mixed Convection Flow," *Journal of Mechanical Science and Technology*, **28**(5), 1881 - 1885.  
<http://dx.doi.org/10.1007/s12206-015-0153-7>
- El-Aziz, M A, 2010, "Flow and Heat Transfer over an Unsteady Stretching Surface with Hall Effect," *Meccanica*, **45**, 97-109.  
<https://doi.org/10.1007/s11012-009-9227-x>
- El-Aziz, M A., 2009, "Viscous Dissipation Effect on Mixed Convection Flow of a Micropolar Fluid over an Exponentially Stretching Sheet," *Can. J. Phys.*, **87**, 359-368.  
<https://doi.org/10.1139/P09-047>
- Hussain, T., Shehzad, S A., Hayat T., Alsaedi, A., Al-Solamy F., and Ramzan, R., 2014, "Radiative Hydromagnetic Flow of Jeffrey Nanofluid by an Exponentially Stretching Sheet," *PLUS One*, **9**(8), No.e103719.  
<https://doi.org/10.1371/journal.pone.0103719>
- Kameswaran, P.K, Narayana, M., Sibanda, P. and Makanda, G., 2012, "On Radiation Effects on Hydromagnetic Newtonian Liquid Flow due to

an Exponential Stretching Sheet,” *Boundary Value Problems*, **2012**, article No. 105, 1-16.

<https://doi.org/10.1186/1687-2770-2012-105>

Kumari, M. and Nath, G., 2014, “Steady Mixed Convection Flow of Maxwell Fluid over an Exponentially Stretching Vertical Surface with Magnetic Field and Viscous Dissipation,” *Meccanica*, **49**, 1263-1274.

<https://doi.org/10.1007/s11012-014-9884-2>

Crane, L J., 1970, “Flow Past a Stretching Plate,” *Journal of Applied Mathematics and Physics*, **21**(4), 645-647.

<https://doi.org/10.1007/BF01587695>

Ibrahim, W., and Shankar, B., 2016, “The Effects of Thermal Radiation and Non-uniform Heat Source/Sink on Stretching Sheet Embedded in Non-Darcian Porous Medium,” *Frontiers in Heat and Mass Transfer*, **7**, 37, 1-8.

<https://doi.org/10.5098/hmt.7.37>

Mabood, F., Khan W A., and Ismail, AI Md., 2014, “MHD Flow over Exponential Radiating Stretching Sheet using Homotopy Analysis Method,” *Journal of King Saud University – Engineering Sciences* (article in press)

<doi.org/10.1016/j.jksues.2014.06.001>.

Magyari E., and Keller, B., 1999, “Heat and Mass Transfer in the Boundary Layers on an Exponentially Stretching Continuous Surface,” *Journal of Physics D: Applied Physics*, **32**, 577-585.

<http://stacks.iop.org/0022-3727/32/i=5/a=012>

Mandal, I.C., and Mukhopadhyay, S., 2013, “Heat Transfer Analysis for Fluid Flow over an Exponentially Stretching Porous Sheet with Surface Heat Flux in Porous Medium,” *Ain Shams Engineering Journal*, **4**, 103–110.

<https://doi.org/10.1016/j.asej.2012.06.004>

Motsa S.S and Shateyi, S., 2006, “Successive Linearisation Solution of Free Convection Non-Darcy Flow with Heat and Mass Transfer,” *Advanced Topics in Mass Transfer*, **19**, 425-438.

<https://doi.org/10.5772/14519>

Mukhopadhyay, S. and Gorla, R.S.R., 2012, “Effects of Partial Slip on Boundary Layer Flow Past a Permeable Exponential Stretching Sheet in Presence of Thermal Radiation,” *Heat Mass Transfer*, **48**, 1773-1781.

<https://doi.org/10.1007/s00231-012-1024-8>

Murthy, P.V.S.N., Ramreddy, Ch. Chamkha, A.J and Rashad, A.M., 2015, “Significance of Viscous Dissipation and Chemical Reaction on Convective Transport in a Boundary Layer Stagnation Point Flow Past a Stretching/Shrinking Sheet in a Nanofluid,” *Journal of Nanofluids*, **4**, 214-222. <https://doi.org/10.1166/jon.2015.1136>

Qasim, M., Hayat, T. and Hendi, A.A., 2011, “Effects of Slip Conditions on Stretching Flow with Ohmic Dissipation and Thermal Radiation,” *Heat Transfer - Asian research*, **40**(7), 641–654.

<https://doi.org/10.1002/hjt.20367>

Sakiadis, B.C., 1961, “Boundary-Layer Equations for Two-Dimensional and Axisymmetric Flow,” *AIChE. Journal*, **7**(1), 26-28. <https://doi.org/10.1002/aic.690070108>

Sakiadis, B.C , 1961, “The Boundary Layer on a Continuous Flat Surface,” *AIChE. Journal*, **7**(2), 221-225.

<https://doi.org/10.1002/aic.690070211>

Santhosh, C., Singh S., and Susheela, C., 2015, “Thermal Radiation in Effects on MHD Boundary Layer Flow over an Exponentially Stretching Surface,” *Applied Mathematics*, **6**, 295-303.

<https://doi.org/10.4236/am.2015.62027>

Seini Y.I., and Makinde,O.D., 2013, “MHD Boundary Layer Flow due to Exponential Stretching Surface with Radiation and Chemical Reaction,” *Mathematical Problems in Engineering*, **2013**.

<http://dx.doi.org/10.1155/2013/163614>

Shateyi, S., and Motsa, S.S., 2011, “Boundary Layer Flow and Double Diffusion over an Unsteady Stretching Surface with Hall Effect,” *Chemical Engineering Communications*, **198**, 1545-1565.

<http://dx.doi.org/10.1080/00986445.2011.555488>

Sparrow E.M and Cess, R.D., 1978, *Radiation Heat Transfer*, Washington, DC: Hemisphere.

Srinivasacharya, D., and Kaladhar, K., 2012, “Mixed Convection Flow of Couple Stress Fluid Between Parallel Vertical Plates with Hall and Ion-Slip Effects,” *Commun Nonlinear Sci Numer Simulat*, **7**, 2447-2462.

<https://doi.org/10.1016/j.cnsns.2011.10.006>

Srinivasacharya, D., and Jagadeeshwar, P., 2017, “Slip Viscous Flow Over an Exponentially Stretching Porous Sheet with Thermal Convective Boundary Conditions,” *Int. J. Appl. Comput. Math*, **3**(4), 3525-3537.

<https://doi.org/10.1007/s40819-017-0311-y>

Srinivasacharya, D., and Jagadeeshwar, P., 2017, “MHD Flow with Hall Current and Joule Heating Effects over an Exponentially Stretching Sheet,” *Nonlinear Engineering-Modeling and Application*, **6**(2), 101-114.

<https://doi.org/10.1515/nleng-2016-0035>

Su X., and Zheng, L., 2013, “Hall Effect on MHD Flow and Heat Transfer of Nanofluids over a Stretching Wedge in the Presence of Velocity Slip and Joule Heating,” *Central European Journal of Physics*, **11**(12), 1694-1703.

<https://doi.org/10.2478/s11534-013-0331-0>

Umehaiah., M, Krishnamurthy, M. R., Rudraswamy., N. G., Gireesha., B. J., and Prasannakumara., B. C., 2017, “Nonlinear Radiative Heat Transfer to Carreau Fluid over a Nonlinear Stretching Sheet in a Porous Medium in the Presence of Non-uniform Heat Source/Sink and viscous dissipation,” *Frontiers in Heat and Mass Transfer*, **9**, 4, 1-8.

<http://dx.doi.org/10.5098/hmt.9.4>

Zaib, A., and Shafie, S., 2014, “Thermal Diffusion and Diffusion Thermo Effects on unsteady MHD free convection flow over a stretching surface considering Joule heating and viscous dissipation with thermal stratification, chemical reaction and Hall current,” *Journal of the Franklin Institute*, **351**, 1268-1287.

<https://doi.org/10.1016/j.jfranklin.2013.10.011>